

*Advances in Nuclear Many-Body Theory, June 7 - 10, 2011  
Primošten, Croatia*

Stellar Electron Capture with  
Finite Temperature Relativistic Random Phase Approximation

Yifei Niu

School of Physics, Peking University, China

June 5, 2011

Collaborators:

Jie Meng: School of Physics, Peking University, China

Nils Paar: Physics Department, University of Zagreb, Croatia

Dario Vretenar: Physics Department, University of Zagreb, Croatia

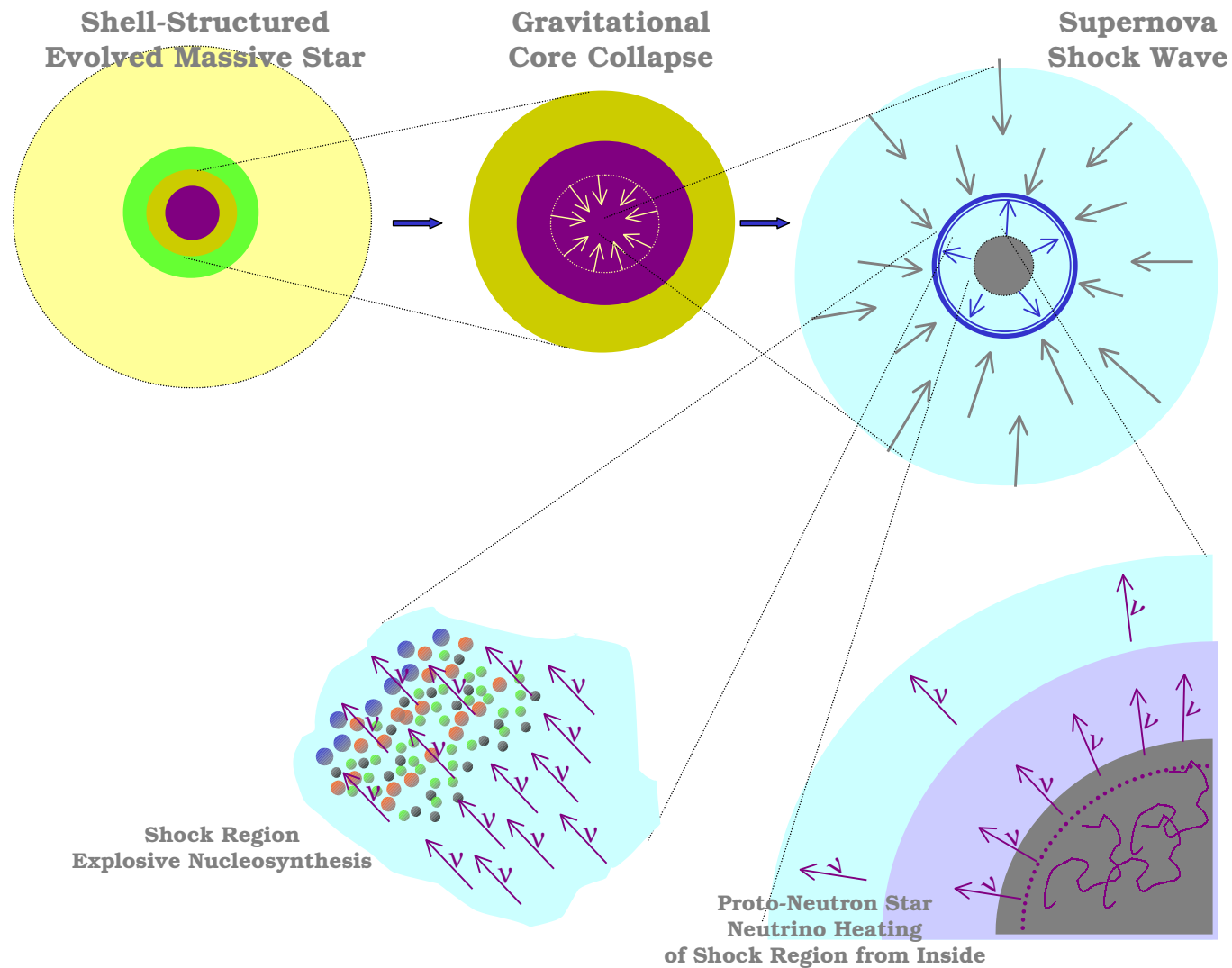
# OUTLINE

- 1 Introduction
- 2 Theory Framework
- 3 Results and discussions
- 4 Summary
- 5 Appendix

# Introduction — Electron capture in stellar evolution

## Collapse of a massive star and a supernova explosion

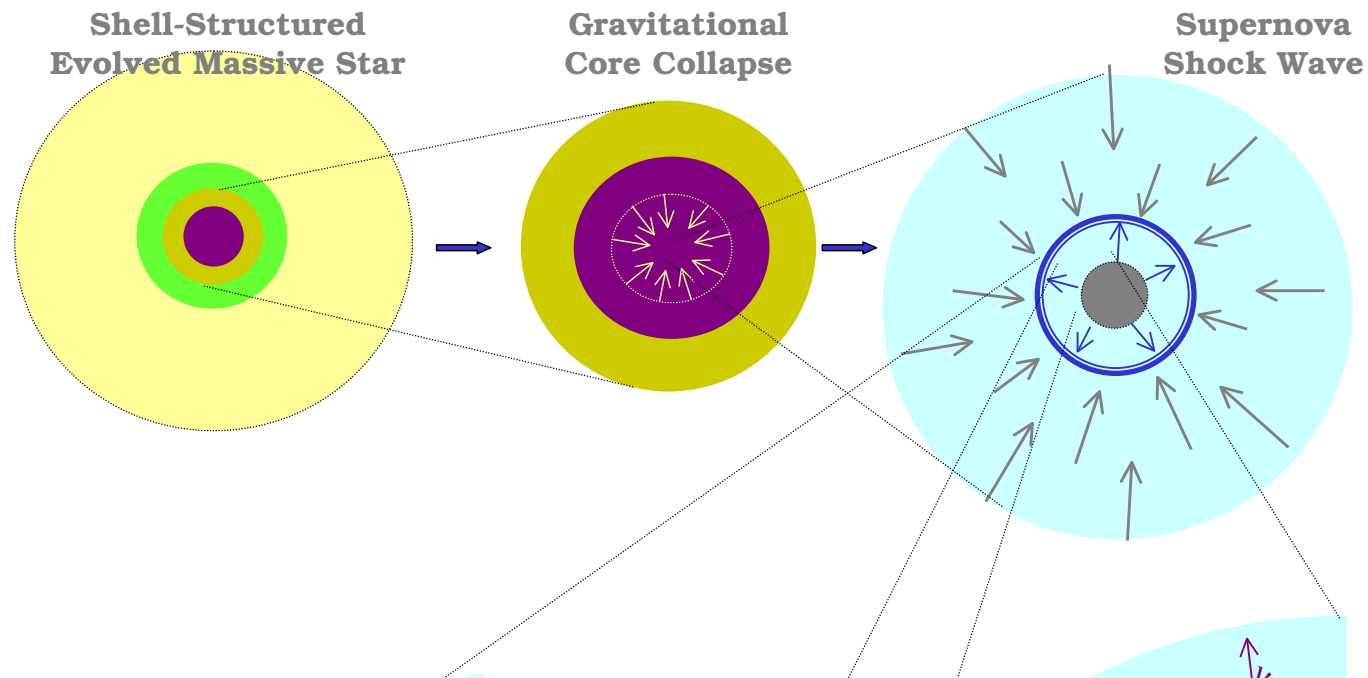
— from Langanke 2008, *Acta Physica Polonica B*, 39.



# Introduction — Electron capture in stellar evolution

## Collapse of a massive star and a supernova explosion

— from Langanke 2008, *Acta Physica Polonica B*, 39.



- The dynamics of core-collapse supernova  $\Leftarrow$   $\left\{ \begin{array}{l} \text{core entropy} \\ \text{lepton to baryon ratio } Y_e \end{array} \right.$
- $\Leftarrow$  weak interaction processes  $\left\{ \begin{array}{l} \beta \text{ decay} \\ \text{electron capture dominate !} \end{array} \right.$

OF SHOCK REGION FROM INSIDE

# Introduction — Electron capture in stellar evolution

## Core Collapse type II supernova

- ◇ initial stage:  $\rho \sim 10^{10}$  g/cm<sup>3</sup>,  $T = 300 - 800$  keV,  $\mu_e$  of the same order as  $Q$  value
  - Electrons are captured by iron range nuclei  $A < 60$ .
  - Electron capture rates are sensitive to detailed GT distribution.
- ◇ higher densities and temperature:  $\mu_e \gg Q$  value
  - Electrons are captured by neutron rich nuclei with  $A > 65$ .
  - Electron capture rates are mainly determined by the total GT strength and centroid energy.
- ◇  $\rho > 10^{11}$  g/cm<sup>3</sup>,  $\mu_e \sim 30$  MeV:
  - Forbidden transitions couldn't be neglected.

# Introduction — Electron capture process

The electron capture on a nucleus  ${}^A_Z X_N$



- Cross section for a transition followed from Fermi's golden rule reads:

$$\frac{d\sigma}{d\Omega} = \frac{1}{(2\pi)^2} V^2 E_\nu^2 \frac{1}{2} \sum_{\text{lepton spins}} \frac{1}{2J_i + 1} \sum_{M_i M_f} |\langle f | \hat{H}_W | i \rangle|^2. \quad (2)$$

$V$ : the quantization volume;  $E_\nu$ : energy of outgoing electron neutrino;  $H_W$ : the Hamiltonian of the weak interaction.

- The evaluation of the matrix elements  $\langle f | \hat{H}_W | i \rangle$  is crucial for the calculation of electron capture cross sections. The initial and final states of nuclei are obtained from nuclear structure models.

# Introduction — Theoretical description

Different nuclear models could be employed to extract information on the initial and final states for the investigation of the stellar electron capture.

- Independent Particle Model (IPM): for  $A = 21 - 60$ 
  - ✓ the first standard tabulation of nuclear weak-interaction rates  
*G. M. Fuller, W. A. Fowler, M. J. Newman, Ap. J. S. 42, 447 1980; 48, 279, 1982;  
G. M. Fuller, W. A. Fowler, M. J. Newman, Ap. J. 252, 715, 1982; 293, 1, 1985.*
- Shell Model Monte Carlo(SMMC): for  $A = 45 - 65$ 
  - ✓ for the first time determines in a microscopic way the Gamow-Teller contributions to the presupernova electron capture rates
  - ✓ take into account thermal effects  
*D. J. Dean, K. Langanke, L. Chatterjee, P. B. Radha, and M. R. Strayer, Phys. Rev. C 58, 536, 1998.*
- Large Scale Shell Model diagonalization (LSSM): for  $A = 45 - 65$ 
  - ✓ an updated tabulation of weak interaction rates
  - ✓ reproduce the experimental  $GT^+$  distributions  
*K. Langanke, G. Martinez-Pinedo, Phys. Lett. B 436, 19, 1998;  
K. Langanke, G. Martinez-Pinedo, Nucl. Phys. A 673, 481, 2000;  
K. Langanke, G. Martinez-Pinedo, At. Data Nucl. Data Tables 79, 1, 2001.*

# Introduction — Theoretical description

RPA approach: more suitable for  $\left\{ \begin{array}{l} \text{the inclusion of forbidden transitions} \\ \text{global calculations of many nuclei} \end{array} \right.$

- Hybrid model (SMMC/RPA): for nuclei with  $Z < 40, N > 40$ 
  - ✓ The SMMC firstly gives the finite temperature occupation numbers, and then the electron capture rates are calculated within the RPA approach.  
*K. Langanke, E. Kolbe, and D. J. Dean, Phys. Rev. C 63, 032801, 2001.*
- QRPA based on Nilsson model with separable Gamow-Teller forces: for  $A = 18 - 100$   
*J. -U. Nabi, and H. V. Klapdor-Kleingrothaus, At. Data Nucl. Data Tables 71, 149, 1999;*  
*J. -U. Nabi, and H. V. Klapdor-Kleingrothaus, At. Data Nucl. Data Tables 88, 237, 2004.*
- QRPA based on Woods-Saxon potential with thermofield dynamics(TFD) formalism  
*A. A. Dzhioev, A. I. Vdovin, V. Y. Ponomarev, J. Wambach, K. Langanke, and G. Martínez-Pinedo, Phys. Rev. C 81, 015804, 2010.*
- finite temperature RPA based on Skyrme functionals
  - ✓ The self-consistent RPA approach is for the first time introduced to the evaluation of electron capture cross sections.  
*N. Paar, G. Colò, E. Khan and D. Vretenar, Phys. Rev. C 80, 055801, 2009.*



# Introduction — Motivation

## Success of covariant density functional

- RMF, RHB : successful for the description of ground-state properties in nuclei all over the periodic table, including those far away from the stability line.

*P. Ring, Prog. Part. Nucl. Phys. 37, 193, 1996.*

*D. Vretenar, A. V. Afanasjev, G. A. Lalazissis and P. Ring, Phys. Rep. 409, 101, 2005.*

*J. Meng, H. Toki, S. G. Zhou, S. Q. Zhang, W. H. Long, and L. S. Geng, Prog. Part. Nucl. Phys. 57, 470, 2006.*

- Relativistic RPA (RRPA): giant resonances, spin isospin resonances

*Z. Y. Ma, V. Giai Nguyen, A. Wandelt D. Vretenar and P. Ring, Nucl. Phys. A 686, 173, 2001.*

*P. Ring, Z. Y. Ma, V. Giai Nguyen, D. Vretenar, A. Wandelt and L. G. Cao, Nucl. Phys. A 694, 249, 2001.*

*T. Nikšić, D. Vretenar, and P. Ring, Phys. Rev. C 66, 064302, 2002.*

*N. Paar, P. Ring, T. Nikšić and D. Vretenar, Phys. Rev. C 67, 034312, 2003.*

*N. Paar, T. Nikšić, D. Vretenar, and P. Ring, Phys. Rev. C 69, 054303, 2004.*

*H. Z. Liang, V. Giai Nguyen, and J. Meng, Phys. Rev. Lett. 101, 122502, 2008.*

- finite temperature RRPA: new low-lying structure of dipole response

*Y.F. Niu, N. Paar, D. Vretenar and J. Meng, Phys. Lett. B 681, 315, 2009.*

## In this work

Investigate the stellar electron capture cross sections and rates based on finite temperature RRPA with the inclusion of multipole transitions.

*Y.F. Niu, N. Paar, D. Vretenar and J. Meng, Phys.Rev. C 83, 045807, 2011.*

# PN-RRPA at finite temperature

- Proton-neutron RPA equations at finite temperature

$$\begin{pmatrix} A_{pnp'n'}^J & B_{pnp'n'}^J \\ -B_{pnp'n'}^J & -A_{pnp'n'}^J \end{pmatrix} \begin{pmatrix} X_{p'n'}^J \\ Y_{p'n'}^J \end{pmatrix} = \omega_\nu \begin{pmatrix} X_{pn}^J \\ Y_{pn}^J \end{pmatrix},$$

where  $A$  and  $B$  are the matrix elements of particle-hole residual interactions:

$$\begin{aligned} A_{pnp'n'}^J &= (\epsilon_p - \epsilon_{\bar{h}}) \delta_{pp'} \delta_{nn'} + V_{pn'n p'}^J (\tilde{u}_p \tilde{v}_n \tilde{u}_{p'} \tilde{v}_{n'} + \tilde{v}_p \tilde{u}_n \tilde{v}_{p'} \tilde{u}_{n'}) (f_{n'} - f_{p'}) \\ B_{pnp'n'}^J &= V_{pn'n p'}^J (\tilde{u}_p \tilde{v}_n \tilde{v}_{p'} \tilde{u}_{n'} + \tilde{v}_p \tilde{u}_n \tilde{u}_{p'} \tilde{v}_{n'}) (f_{p'} - f_{n'}), \end{aligned}$$

- Occupation probability:  $f_i = [1 + \exp(\frac{\epsilon_i - \mu}{kT})]^{-1}$ , and we define

$$\begin{aligned} \tilde{u}_p &= 0, & \tilde{v}_p &= 1, & \tilde{u}_n &= 1, & \tilde{v}_n &= 0, & \text{when } f_p > f_n & (\bar{p}n); \\ \tilde{u}_p &= 1, & \tilde{v}_p &= 0, & \tilde{u}_n &= 0, & \tilde{v}_n &= 1, & \text{when } f_p < f_n & (p\bar{n}). \end{aligned}$$

- Normalization

$$\sum_{pn} [(X_{pn}^{J\nu})^2 - (Y_{pn}^{J\nu})^2] |f_p - f_n| = 1$$

- Transition strength

$$B_{J\nu}^{T-} = \left| \sum_{pn} (X_{pn}^{J\nu} \tilde{u}_p \tilde{v}_n + Y_{pn}^{J\nu} \tilde{v}_p \tilde{u}_n) \langle p || T_- || n \rangle |f_n - f_p| \right|^2,$$

$$B_{J\nu}^{T+} = \left| \sum_{pn} (X_{pn}^{J\nu} \tilde{v}_p \tilde{u}_n + Y_{pn}^{J\nu} \tilde{u}_p \tilde{v}_n) \langle p || T_+ || n \rangle |f_n - f_p| \right|^2.$$

# Electron capture rate

- Rate

$$\lambda_{ec} = \frac{1}{\pi^2 \hbar^3} \int_{E_e^0}^{\infty} p_e E_e \sigma_{ec}(E_e) f(E_e, \mu_e, T) dE_e \quad (3)$$

where  $E_e^0 = \max(|Q_{if}|, m_e c^2)$ ,  $Q_{if} = -E_{\text{RPA}} - \Delta_{np}$ , and  $p_e = (E_e^2 - m_e^2 c^4)^{1/2}$ .  
Electron distribution in stellar environment

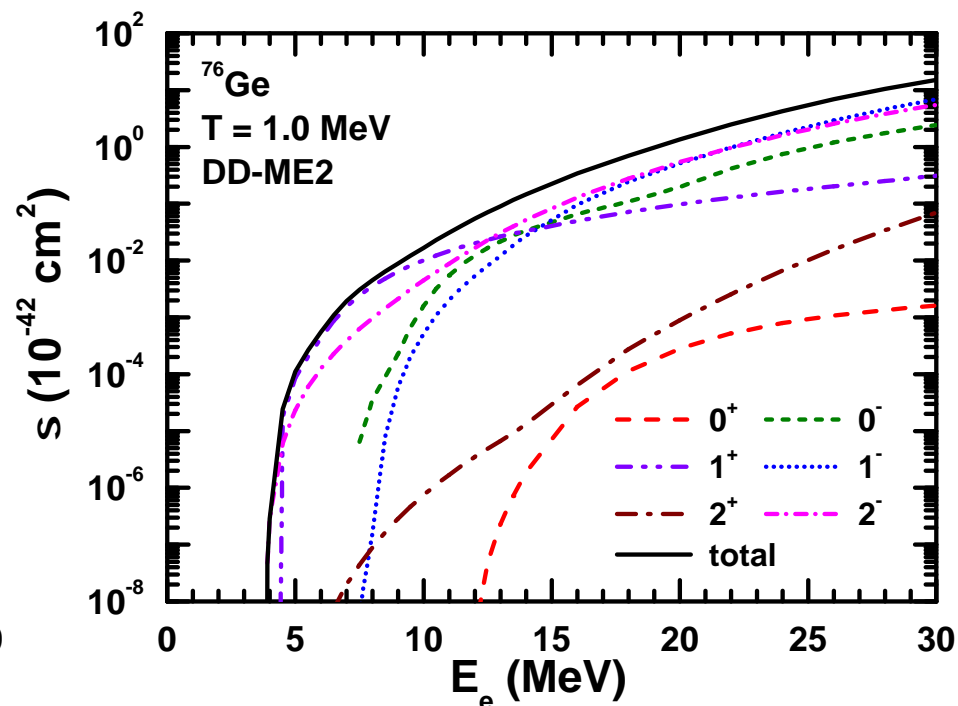
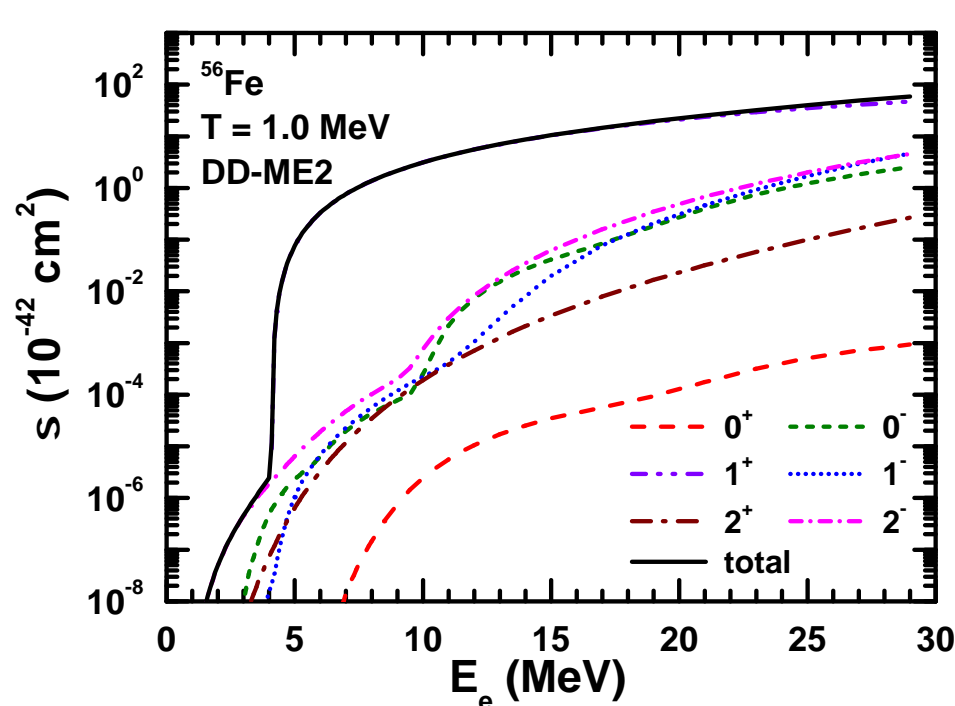
$$f(E_e, \mu_e, T) = \frac{1}{\exp\left(\frac{E_e - \mu_e}{kT}\right) + 1} \quad (4)$$

where the chemical potential is determined from the density  $\rho$  by inverting the relation

$$\rho Y_e = \frac{1}{\pi^2 N_A} \left(\frac{m_e c}{\hbar}\right)^3 \int_0^{\infty} (f_e - f_{e+}) p^2 dp \quad (5)$$

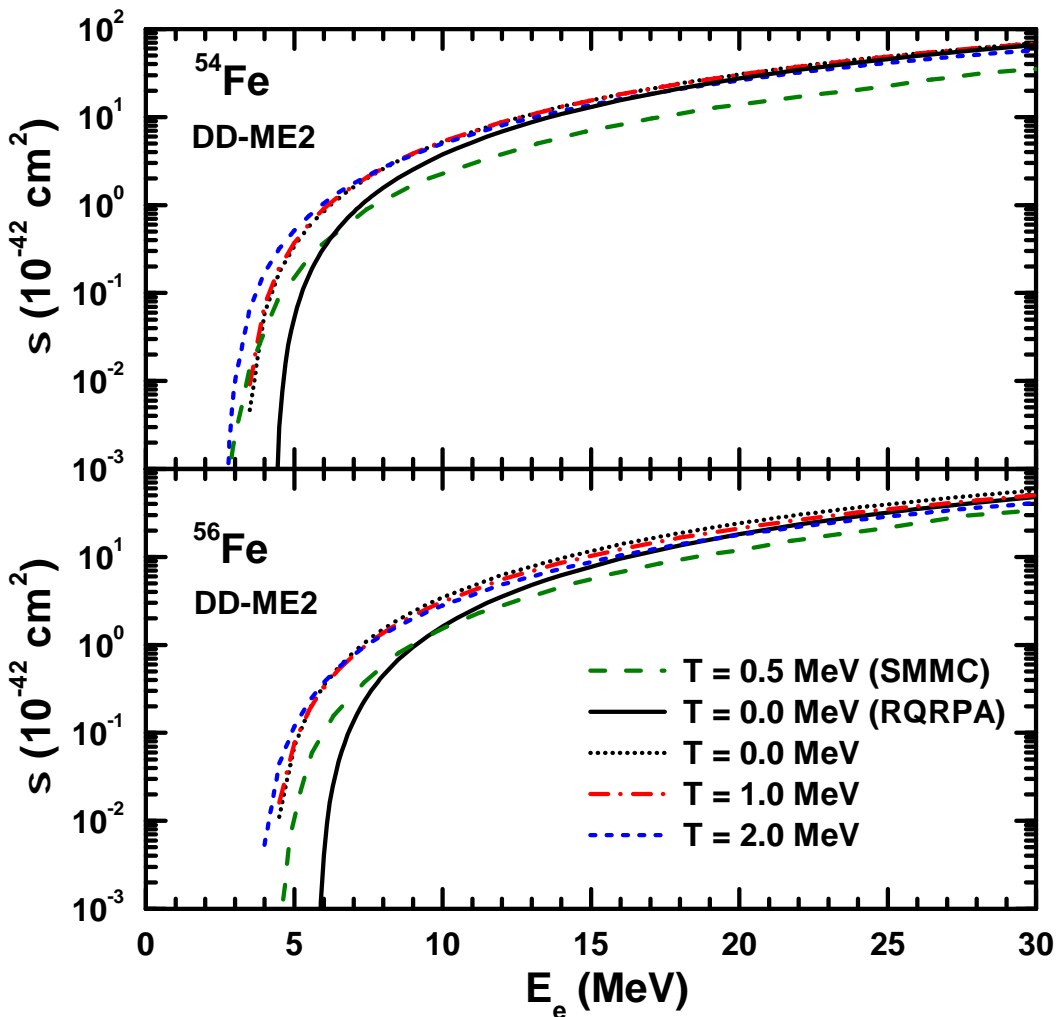
$Y_e$ : the ratio of the number of electrons to the number of baryons;  $N_A$ : Avagadro's number;  $f_e, f_{e+}$ : electron and positron distribution.

# Contributions from different $J^\pi$ excitations



- For <sup>56</sup>Fe, 1<sup>+</sup> (i.e. GT<sup>+</sup>) gives almost all the contributions to cross section all the way up to  $E_e = 30$  MeV. In the other components of excitations, the first forbidden transitions (0<sup>-</sup>, 1<sup>-</sup>, 2<sup>-</sup>) are more important.
- For neutron rich nucleus <sup>76</sup>Ge, the first forbidden transitions start to give more contributions than 1<sup>+</sup> from  $E_e \simeq 12$  MeV.

# Electron capture cross section

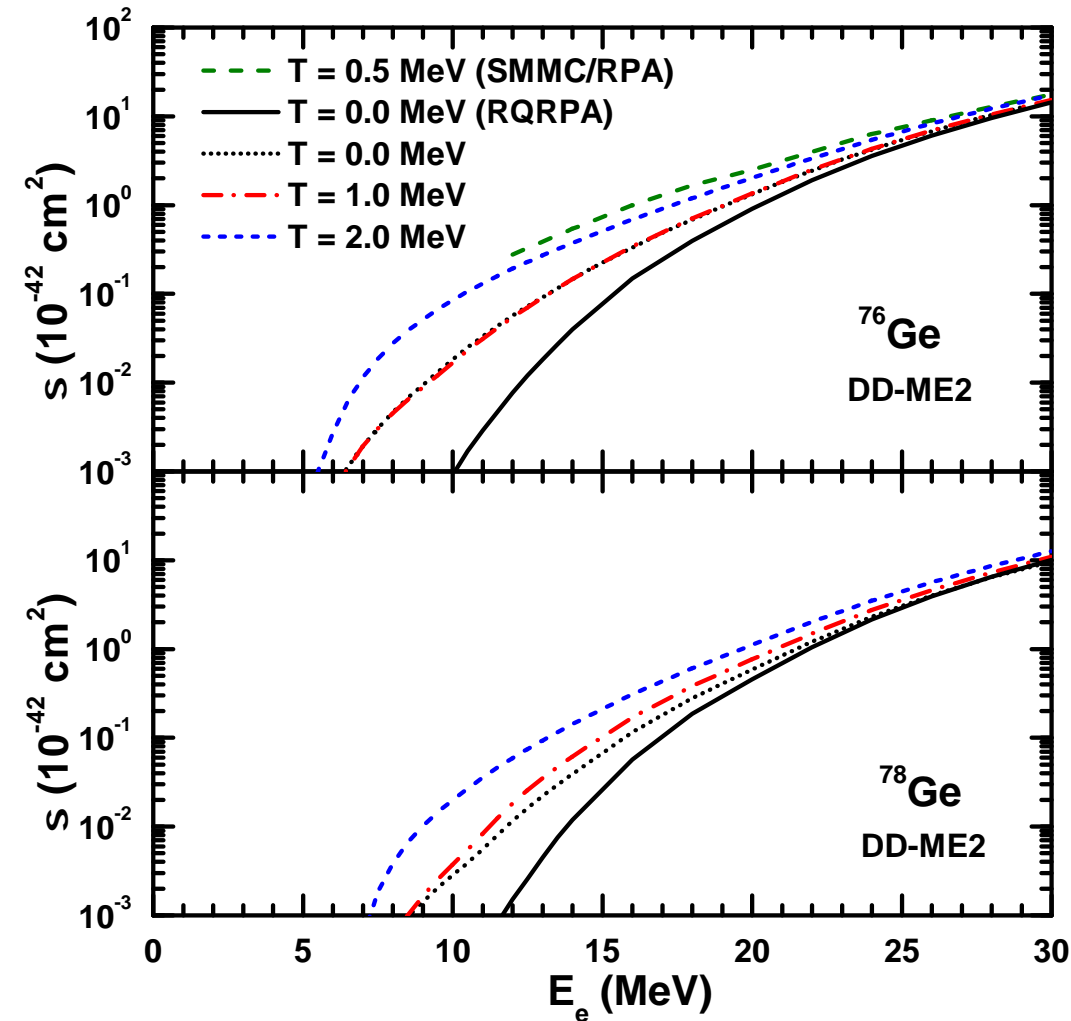


$$\sigma_{ec} \propto E_\nu^2$$

$$E_\nu = E_e - E_{\text{RPA}} - \Delta_{NP}$$

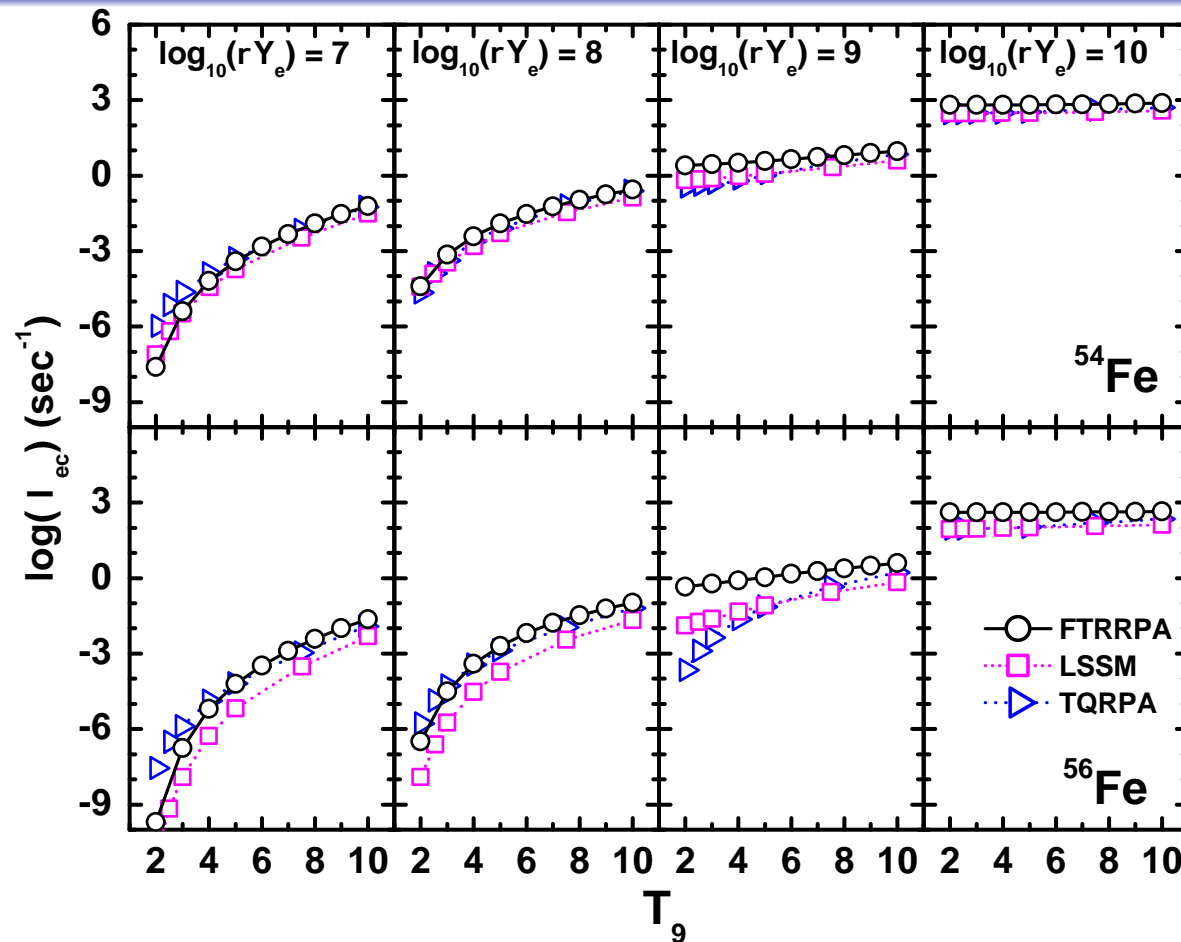
- Threshold energy for electron capture is lowered with increased temperature.
- Cross section is less dependent on temperature at high electron energies.
- Threshold energies increase and cross sections decrease with neutron number.
- difference with SMMC:  
GT distribution

# Electron capture cross section



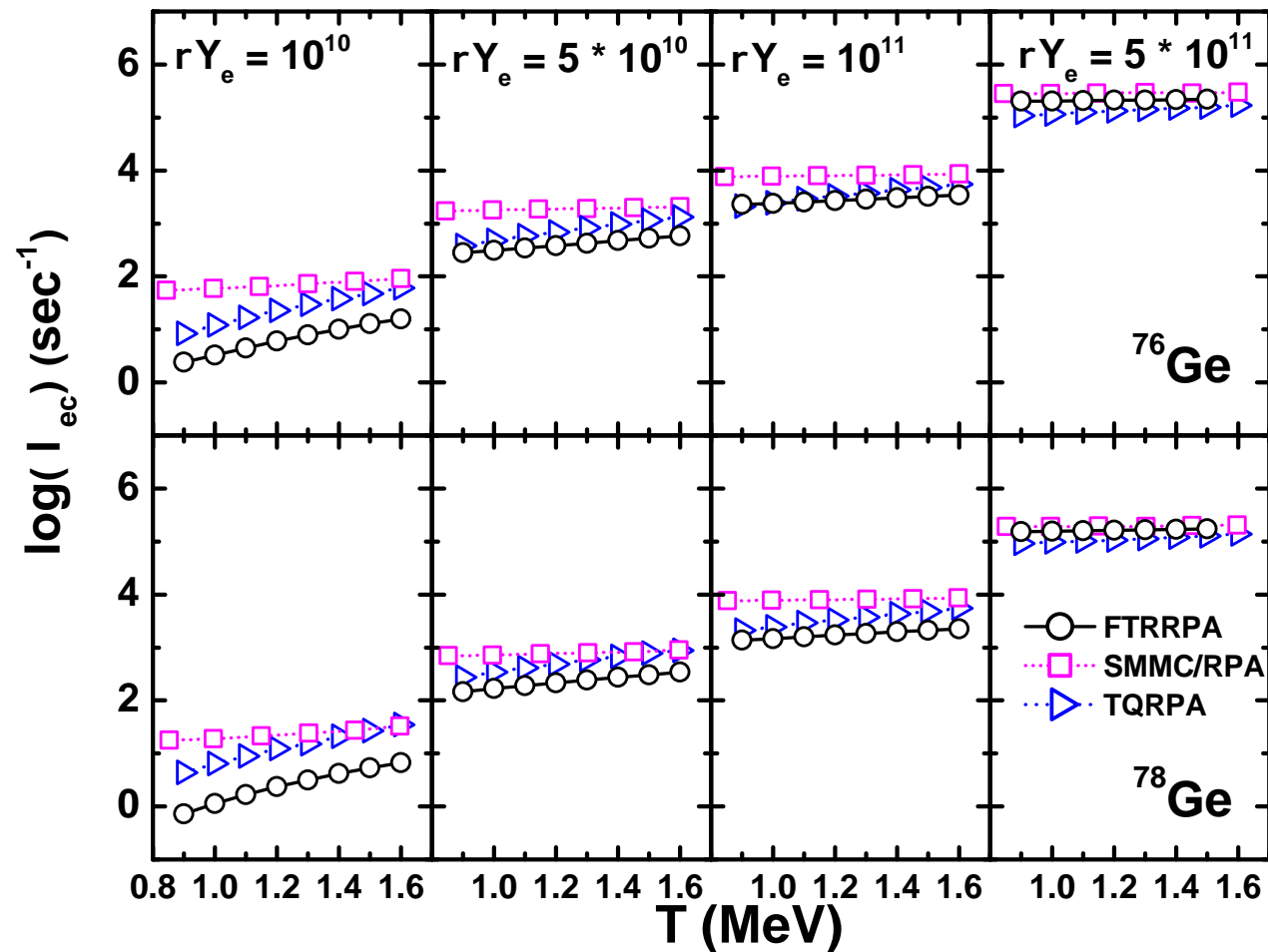
- Cross sections are reduced by an order of magnitude compared to irons, but similar evolution with temperature is found.
- strong temperature dependence at  $E_e \leq 12 \text{ MeV}$ .
- SMMC/RPA predicts larger cross sections due to the strong configuration mixing.

# Electron capture rate



- Electron capture rates increase with temperature and the electron densities.
  - In high electron densities, it increases more slowly.
- similar trend of temperature dependence as shell model
  - better agreement in  $^{54}\text{Fe}$  than  $^{56}\text{Fe}$
  - $\rho Y_e = 10^9 \text{ g/cm}^3$ :  $\lambda_e \sim 5 \text{ MeV}$ , close to threshold energy  $\Rightarrow$  sensitive to detailed GT distribution  $\Rightarrow$  larger discrepancy

# Electron capture rate



- similar behavior with temperature and electron density as Fe
- more similar temperature dependence as TQRPA
  - lower densities: strong temperature dependence.  $\lambda_e \sim 11$  MeV, dominated by GT
  - larger densities: less sensitive to temperature.  $\lambda_e \sim 23$  MeV, dominated by forbidden transitions



# Summary & Perspectives

The electron capture cross sections and rates in stellar environment, including multipole excitations, are calculated based on self-consistent finite temperature PN-RRPA.

- In the calculation of cross sections, the  $GT^+$  transitions provide major contribution for  $^{54,56}\text{Fe}$ , whereas for  $^{76,78}\text{Ge}$  forbidden transitions play an important role at  $E_e > 10$  MeV.
- The principal effect of increasing temperature is the lowering of the electron-capture threshold energy. For  $^{76,78}\text{Ge}$  the cross sections in the low-energy region are very sensitive to temperature.
- In the calculation of capture rates, for  $^{54,56}\text{Fe}$  FTRRPA displays a similar trend as shell model. For  $^{76,78}\text{Ge}$ , the temperature dependence in FTRRPA is very close to TQRPA, whereas the dependence is much weaker in the hybrid model.

Perspectives:

- for open-shell nuclei at very low temperatures: pairing correlations
- the inclusion of higher-order correlations beyond the RPA level

# Acknowledgements

## Collaborators:

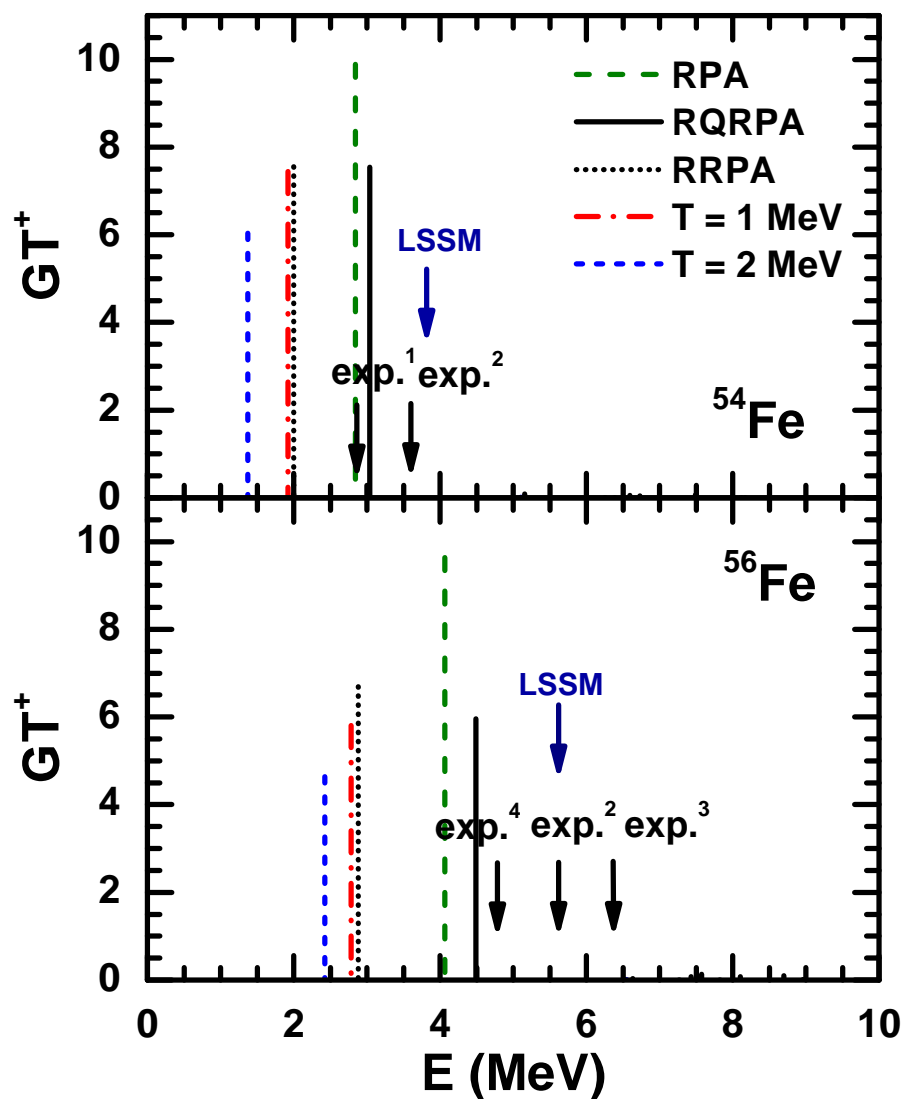
Jie Meng: School of Physics, Peking University, China

Nils Paar: Physics Department, University of Zagreb, Croatia

Dario Vretenar: Physics Department, University of Zagreb, Croatia

*THANK YOU !*

# Evolution of $GT^+$ with temperature



- Pairing correlations shift the transition to higher energy, because additional energy is needed to break a proton pair.
- From  $T=0$  (RQRPA) to  $T=1$ , energy decreases due to pairing collapse.
- From  $T=1$  to  $T=2$ , energy decreases due to softening of the repulsive residual interaction.
- Transition strength becomes weaker with increasing temperature or with pairing by the partial occupation factors.

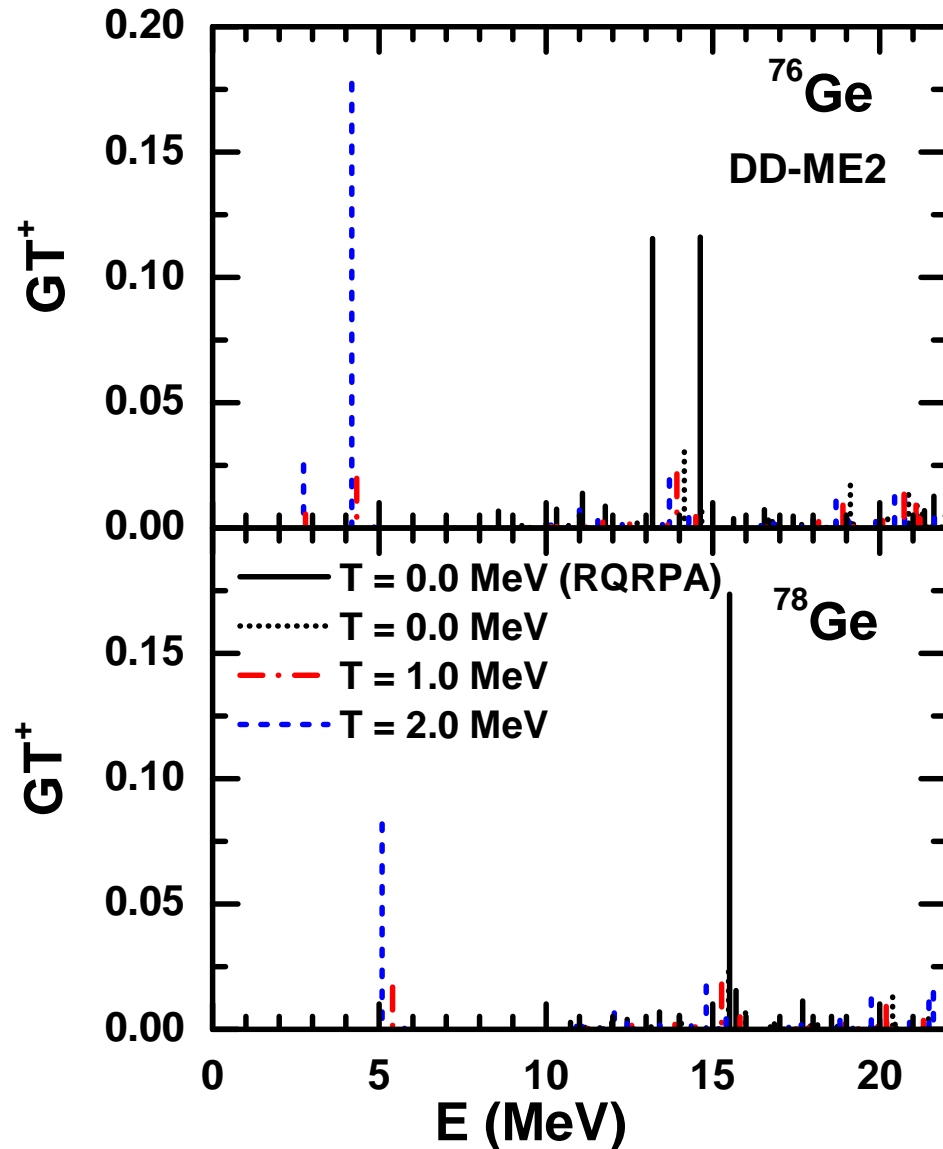
[1] M. C. Vetterli, et. al. *Phys. Rev. C* 40, 559, 1989.

[2] T. Rönqvist, et. al. *Nucl. Phys. A* 563, 225, 1993.

[3] S. El-Kateb, et. al. *Phys. Rev. C* 49, 3128, 1994.

[4] D. Frekers, *Nucl. Phys. A* 752, 580c, 2005.

# Evolution of $GT^+$ with temperature



- Unblocking mechanisms: pairing correlations & thermal excitations.
- From  $T=0$  (RQRPA) to  $T=1$ :

- energy decreases much
- $T=0$ :

$$\sqrt{(\epsilon_p - \lambda_p)^2 + \Delta_p^2} + \sqrt{(\epsilon_n - \lambda_n)^2 + \Delta_n^2}$$

$T=1$ :  $\epsilon_n - \epsilon_p$ .

- strength decreases much
- pairing correlation  $\Rightarrow$  more diffused fermi surface
- From  $T=1$  to  $T=2$ : energy decreases a little while strength is enhanced a lot.

# Electron capture cross section

The electron capture on a nucleus  ${}^A_Z X_N$



- Cross section for a transition between initial state  $|i\rangle$  and a final state  $|f\rangle$  followed from Fermi's golden rule reads:

$$\frac{d\sigma}{d\Omega} = 2\pi |\langle f | \hat{H}_W | i \rangle|^2 V \frac{E_\nu^2 dE_\nu}{(2\pi)^3} \delta(W_f - W_i) / \frac{1}{V}, \quad (7)$$

where  $V \frac{E_\nu^2 dE_\nu}{(2\pi)^3}$  is the number of neutrino states in the interval  $E_\nu \sim E_\nu + dE_\nu$ , and electron flux is  $1/V$ .  $\delta(W_f - W_i)$  means the energy conservation.

- Average the initial states and sum over all the final states for a specific nuclear excitation state  $f$ :

$$\begin{aligned} \frac{d\sigma}{d\Omega} &= \frac{1}{2J_i + 1} \sum_{M_i} \frac{1}{2} \sum_{\text{lepton spins}} \sum_{M_f} \int dE_\nu 2\pi |\langle f | \hat{H}_W | i \rangle|^2 V \frac{E_\nu^2}{(2\pi)^3} \delta(W_f - W_i) / \frac{1}{V} \\ &= \frac{1}{(2\pi)^2} V^2 E_\nu^2 \frac{1}{2} \sum_{\text{lepton spins}} \frac{1}{2J_i + 1} \sum_{M_i M_f} |\langle f | \hat{H}_W | i \rangle|^2. \end{aligned} \quad (8)$$

# Electron capture cross section

- The Hamiltonian of the weak interaction  $H_W$  is expressed in the standard current-current form, i.e., in terms of the nuclear  $\mathcal{J}_\lambda$  and lepton  $j_\lambda$  currents.

$$H_W = -\frac{G}{\sqrt{2}} \int d^3x \mathcal{J}_\lambda(\mathbf{x}) j_\lambda(\mathbf{x}) \quad (9)$$

$G$ : weak coupling constant.

- Denoting the appropriate leptonic matrix element by  $l_\mu e^{-i\mathbf{q}\cdot\mathbf{x}}$ , the resulting transition matrix element reads

$$\begin{aligned} \langle f | \hat{H}_W | i \rangle &= -\frac{G}{\sqrt{2}} l_\mu \int d\mathbf{x} e^{-i\mathbf{q}\cdot\mathbf{x}} \langle f | \mathcal{J}_\mu(\mathbf{x}) | i \rangle \\ &= -\frac{G}{\sqrt{2}} \int d\mathbf{x} e^{-i\mathbf{q}\cdot\mathbf{x}} [\mathbf{l} \cdot \mathcal{J}(\mathbf{x})_{fi} - l_0 \mathcal{J}_0(\mathbf{x})_{fi}]. \end{aligned} \quad (10)$$

$\mathbf{q} = \mathbf{p}_\nu - \mathbf{p}_l$ : the momentum transfer.

# Electron capture cross section

Making use of the expansion

$$e^{i \mathbf{q} \cdot \mathbf{x}} = \sum_{J=0}^{\infty} [4\pi(2J+1)]^{1/2} i^J j_J(\kappa x) Y_{J0}(\Omega_x), \quad (11)$$

$$\mathbf{e}_{q\lambda} e^{i \mathbf{q} \cdot \mathbf{x}} = -\frac{i}{\kappa} \sum_{J=0}^{\infty} [4\pi(2J+1)]^{1/2} i^J \nabla (j_J(\kappa x) Y_{J0}(\Omega_x)), \quad \text{for } \lambda = 0, \quad (12)$$

$$= -\sum_{J \geq 1}^{\infty} [2\pi(2J+1)]^{1/2} i^J [\lambda j_J(\kappa x) \mathcal{Y}_{JJ1}^{\lambda} + \frac{1}{\kappa} \nabla \times (j_J(\kappa x) \mathcal{Y}_{JJ1}^{\lambda})], \quad \text{for } \lambda = \pm 1, \quad (13)$$

where  $\mathcal{Y}_{JJ1}^M = \sum_{m\lambda} \langle lm1\lambda | 1JM \rangle Y_{lm}(\theta, \phi) \mathbf{e}_{\lambda}$ , the transition matrix elements could become

$$\begin{aligned} \langle f | \hat{H}_W | i \rangle &= -\frac{G}{\sqrt{2}} \langle f | \left\{ -\sum_{\lambda=\pm 1} l_{\lambda} \sum_{J \geq 1}^{\infty} [2\pi(2J+1)]^{1/2} (-i)^J [\lambda \hat{T}_{J-\lambda}^{mag}(\kappa) + \hat{T}_{J-\lambda}^{el}(\kappa)] \right. \\ &\quad \left. + \sum_{J=0}^{\infty} [4\pi(2J+1)]^{1/2} (-i)^J [l_3 \hat{\mathcal{L}}_{J0}(\kappa) - l_0 \hat{\mathcal{M}}_{J0}(\kappa)] \right\} | i \rangle, \end{aligned} \quad (14)$$

# Electron capture cross section

where the multipole operators are defined by

$$\hat{\mathcal{M}}_{JM}(\kappa) = \hat{M}_{JM} + \hat{M}_{JM}^5 = \int d\mathbf{x} [j_J(\kappa x) Y_{JM}(\Omega_x)] \hat{\mathcal{J}}_0(\mathbf{x}), \quad (15)$$

$$\hat{\mathcal{L}}_{JM}(\kappa) = \hat{L}_{JM} + \hat{L}_{JM}^5 = \frac{i}{\kappa} \int d\mathbf{x} [\nabla (j_J(\kappa x) Y_{JM}(\Omega_x))] \cdot \hat{\mathcal{J}}(\mathbf{x}), \quad (16)$$

$$\hat{\mathcal{T}}_{JM}^{el}(\kappa) = \hat{T}_{JM}^{el} + \hat{T}_{JM}^{el5} = \frac{1}{\kappa} \int d\mathbf{x} [\nabla \times (j_J(\kappa x) \mathcal{Y}_{JJ1}^M)] \cdot \hat{\mathcal{J}}(\mathbf{x}), \quad (17)$$

$$\hat{\mathcal{T}}_{JM}^{mag}(\kappa) = \hat{T}_{JM}^{mag} + \hat{T}_{JM}^{mag5} = \int d\mathbf{x} [(j_J(\kappa x) \mathcal{Y}_{JJ1}^M)] \cdot \hat{\mathcal{J}}(\mathbf{x}). \quad (18)$$



# Electron capture cross section

Making use of the Wigner-Eckart theorem

$$\langle J_f M_f | \mathcal{T}_{JM} | J_i M_i \rangle = (-)^{J_f - M_f} \begin{pmatrix} J_f & J & J_i \\ -M_f & M & M_i \end{pmatrix} \langle J_f || \mathcal{T}_J || J_i \rangle \quad (19)$$

and the orthogonality relation of  $3j$  coefficients

$$\frac{1}{2J_i + 1} \sum_{M_f} \sum_{M_i} \begin{pmatrix} J_f & J & J_i \\ -M_f & M & M_i \end{pmatrix} \begin{pmatrix} J_f & J' & J_i \\ -M_f & M' & M_i \end{pmatrix} = \delta_{JJ'} \delta_{MM'} \frac{1}{2J + 1} \frac{1}{2J_i + 1}, \quad (20)$$

we could get

$$\begin{aligned} & \frac{1}{2J_i + 1} \sum_{M_f} \sum_{M_i} |\langle f | \hat{H}_W | i \rangle|^2 \\ &= \frac{G^2}{2} \frac{1}{2J_i + 1} \left\{ \sum_{\lambda=\pm 1} l_\lambda l_\lambda^* \sum_{J \geq 1} 2\pi |\langle J_f || \lambda \mathcal{T}_J^{mag} + \mathcal{T}_J^{el} || J_i \rangle|^2 \right. \\ & \quad \left. + \sum_{J \geq 0} 4\pi [l_3 l_3^* |\langle J_f || \mathcal{L}_J || J_i \rangle|^2 + l_0 l_0^* |\langle J_f || \mathcal{M}_J || J_i \rangle|^2 - 2\text{Re} l_3 l_0^* \langle J_f || \mathcal{L}_J || J_i \rangle \langle J_f || \mathcal{M}_J || J_i \rangle^*] \right\}. \end{aligned} \quad (21)$$

# Electron capture cross section

Until now, the electron capture cross section has the form

$$\begin{aligned}
 \frac{d\sigma}{d\Omega} &= \frac{1}{(2\pi)^2} V^2 E_\nu^2 \frac{1}{2} \sum_{\text{lepton spins}} \frac{1}{2J_i + 1} \sum_{M_i M_f} |\langle f | \hat{H}_W | i \rangle|^2 \\
 &= \frac{1}{(2\pi)^2} V^2 E_\nu^2 \frac{1}{2} \sum_{\text{lepton spins}} \frac{G^2}{2} \frac{1}{2J_i + 1} \left\{ \sum_{\lambda=\pm 1} l_\lambda l_\lambda^* \sum_{J \geq 1} 2\pi |\langle J_f || \lambda \mathcal{T}_J^{\text{mag}} + \mathcal{T}_J^{\text{el}} || J_i \rangle|^2 \right. \\
 &\quad \left. + \sum_{J \geq 0} 4\pi [l_3 l_3^* |\langle J_f || \mathcal{L}_J || J_i \rangle|^2 + l_0 l_0^* |\langle J_f || \mathcal{M}_J || J_i \rangle|^2 - 2\text{Re} l_3 l_0^* \langle J_f || \mathcal{L}_J || J_i \rangle \langle J_f || \mathcal{M}_J || J_i \rangle^*] \right\}.
 \end{aligned}$$

As the summation of leptonic matrix element on lepton spins could be related to the unit vectors of neutrino momentum  $\hat{\nu} = \mathbf{p}_\nu / |\mathbf{p}_\nu|$ , transfer momentum  $\hat{\mathbf{q}} = \mathbf{q} / |\mathbf{q}|$ , and  $\boldsymbol{\beta} = \mathbf{p}_e / E_e$ , the electron capture cross section finally becomes

$$\begin{aligned}
 \frac{d\sigma}{d\Omega} &= \frac{G^2}{2\pi} \frac{E_\nu^2}{2J_i + 1} \left\{ \sum_{J \geq 0} \left\{ (1 - \hat{\nu} \cdot \boldsymbol{\beta} + 2(\hat{\nu} \cdot \hat{\mathbf{q}})(\boldsymbol{\beta} \cdot \hat{\mathbf{q}})) |\langle J_f || \mathcal{L}_J || J_i \rangle|^2 \right. \right. \\
 &\quad \left. \left. + (1 + \hat{\nu} \cdot \boldsymbol{\beta}) |\langle J_f || \mathcal{M}_J || J_i \rangle|^2 - 2\hat{\mathbf{q}} \cdot (\hat{\nu} + \boldsymbol{\beta}) \text{Re} \langle J_f || \mathcal{L}_J || J_i \rangle \langle J_f || \mathcal{M}_J || J_i \rangle^* \right\} \right. \\
 &\quad \left. + \sum_{J \geq 1} \left\{ (1 - (\hat{\nu} \cdot \hat{\mathbf{q}})(\boldsymbol{\beta} \cdot \hat{\mathbf{q}})) [|\langle J_f || \mathcal{T}_J^{\text{mag}} || J_i \rangle|^2 + |\langle J_f || \mathcal{T}_J^{\text{el}} || J_i \rangle|^2] \right. \right. \\
 &\quad \left. \left. - 2\hat{\mathbf{q}} \cdot (\hat{\nu} - \boldsymbol{\beta}) \text{Re} \langle J_f || \mathcal{T}_J^{\text{mag}} || J_i \rangle \langle J_f || \mathcal{T}_J^{\text{el}} || J_i \rangle^* \right\} \right\}. \tag{22}
 \end{aligned}$$

# Electron capture cross section

- ◇ Allowed Processes: the long-wave limit where  $\kappa = |\mathbf{q}| \rightarrow 0$ .  
The only surviving multipoles in this limit are

$$\mathcal{T}_{1M}^{el} = \frac{i}{\sqrt{6\pi}} F_A \sum_{i=1}^A \tau_{\pm}(i) \boldsymbol{\sigma}(i); \quad \text{Gamow-Teller} \quad (23)$$

$$\mathcal{M}_{00} = \frac{1}{\sqrt{4\pi}} F_1 \sum_{i=1}^A \tau_{\pm}(i); \quad \text{Fermi} \quad (24)$$

## Remarks

- These operators give rise to the allowed weak transitions in the traditional picture of the nucleus.
- The operators and transitions they give rise to are known as Gamow-Teller and Fermi respectively.